1

Biocompatible 3D printed thermoplastic scaffold for osteoblast differentiation of equine iPS cells

Arabella Baird[1], Noelia Dominguez Falcon[2], Aram Saeed[a2], Deborah Jane Guest[a1*]

[1]Animal Health Trust, Lanwades Park, Kentford, Newmarket, Suffolk, CB8 7UU, UK

[2]School of Pharmacy, University of East Anglia, Norwich, NR4 7TJ, UK

[a]These authors share senior authorship

*Corresponding author: Guest, D J (BSc, PhD): Tel; +44(0)1638 751000, Fax; +44(0)1638 555643, email; debbie.guest@aht.org.uk

2

Abstract

Horses, like humans, can experience bone fractures and due to their large size and need to bear weight on all limbs during the recovery period, they can be difficult to treat. Surgical techniques to improve fracture repair are improving, but to date, regenerative medicine technologies to aid fracture healing are not commonly applied in horses.

We have previously demonstrated that equine induced pluripotent stem cells (iPSCs) can be differentiated into bone forming osteoblasts in 2D culture. Here we report on the use of a thermoplastic, 3D printed polymer to provide a scaffold for successful, *in vitro* osteoblast differentiation of equine iPSCs. The scaffold provides a transparent, cost effect solution to allow the analysis of osteoblast differentiation using live cell imaging, immunohistochemistry and quantitative PCR. This *in vitro* study demonstrates the future feasibility of generating 3D bone constructs through the cell seeding of scaffolds to use in regenerative medicine strategies to improve fracture repair in a relevant, large animal model.

Impact statement

Here we describe the use of a cost-effective scaffold that can be used for *in vitro* studies of osteoblast differentiation by stem cells. The scaffolds can be printed to any size and shape, conditioned to improve cell adherence and they are transparent to allow clear visualisation of the cells in culture or post immunohistochemical staining. Osteoblast differentiation of equine iPSCs was successfully performed and analysed on a 3D printed scaffold, which allows the future development of bone constructs to aid fracture repair in horses.

3

Introduction

Fractures caused by bone overloading or direct trauma are a significant welfare issue in multiple horse breeds taking part in a range of different disciplines[1]. Severe fracture leads to euthanasia, whereas smaller fractures can be treated conservatively with box rest and a cast. In delayed union or comminuted fractures surgery is required[2] but up to 40% of horses do not return to their previous athletic activity[3]. Regenerative medicine strategies using bone tissue engineering to improve fracture reunion and recovery would significantly improve horse welfare.

Bone grafts are used to promote bone regeneration and restore normal bone architecture in humans[4], however it is difficult to obtain sufficient tissue without donor site morbidity. In horses, autologous bone grafting has been performed for many years[5,6], but the effects on the donor site can be even more catastrophic, as the loss of tissue can lead to fracture at the donor site as the horse recovers from anaesthesia[7]. Using stem cells to enhance tissue healing is therefore becoming a popular alternative in both species[8-10].

Induced pluripotent stem cells are cells that are derived from somatic adult cells and have been reprogrammed such that they resemble an embryonic-like state and are capable of indefinite proliferation and can form cells from all three germ line lineages (endoderm, ectoderm and mesoderm)[11] including bone-forming osteoblasts[12-14]. We have successfully generated iPSC lines from equines[15] and have developed methods to differentiate the iPSCs into osteoblasts using traditional 2D cell culture techniques[16]. Equine iPSCs may therefore have the potential to provide large numbers of osteoblasts to utilise in tissue engineering strategies to aid fracture repair in horses.

It has been well documented that compared to 2D cultures, 3D systems provide more accurate modelling of the physiological and cellular environment of cells and promote and maintain lineage specific differentiation and normal cellular architecture[17-19]. The use of iPSCs with 3D scaffolds to enhance cell attachment, proliferation and matrix deposition offer a promising option in regenerative medicine and allow cell organisation that is more closely related to native tissues than 2D culture[20]. However, to date there are no reports differentiation of equine iPSCs into osteoblasts on a 3D scaffold.

The overall aim of this study was to assess the potential of a 3D-printed polymer scaffold to support *in vitro* osteoblastic differentiation of equine iPSCs. .

4

Materials and Methods

Thermoplastic 3D printed polymers

Thermoplastic polymers Polycarbonate BendLay 3D Filament, transparent finish (Orbi-Tech) were printed using a Fused Deposition Modelling 3D printer (MakerBot Replicator 2 Desktop 3D Printer). The following printer settings were used: slicing setting was 0.2 mm, travel speed of the extrusion nozzle was 150 mm/s, z-axis speed was 23 mm/s, extruder temperature was 215°C, feeding rate of the filament was 30 mm/s, infill density was 100%, nozzle diameter was 0.4 mm and the filament diameter was 1.77 mm. The pore size was set at 400 μm. The total thickness of the scaffolds was 1.66 mm, with each scaffold layer being 0.2 mm thick. Three different scaffold diameters were tested: 15.14 mm, 14.90 mm and 14.60 mm. Two scaffold types were tested; open scaffolds and closed scaffolds. The only difference between them being the presence of a fine mesh (150 μm pore size) on the base of the closed scaffolds. Where present, a single layer of the fine mesh (0.2 mm thick) was printed as a continuation of the main scaffold.

The scaffold surface was conditioned by oxygen etching using a Bio Rad PT7125 Barrel Plasma Etcher at 150 W, under 2 millibars pressure for 2 hrs to enhance cell adhesion. After printing, the scaffolds were preserved in a sealed container indefinitely at room temperature. After the oxygen etching, the scaffolds were preserved in a sealed container and stored at -20°C degrees until further use, or at 4°C for up to 6 weeks.

Scanning Electron Microscope (SEM)

The scaffolds seeded with 3T3 cells and cultured were fixed with 4% paraformaldehyde solutions in PBS overnight prior to gold coating on the sputter machine. The scaffold samples were loaded on to aluminium stubs with carbon tabs pre-fixed. The samples were gold coated using a Polaron SC7640 sputter coater, manufactured by Quorum Technologies. The coating parameters were 2.2 kV, 20 mA, 55 mm form Au target, 30 sec coating. The coated samples were washed three times with PBS and left to air dry prior to imaging on the Scanning Electron Microscope machine for imaging, (JSM 5900LV manufactured by JEOL fitted with a tungsten filament, acceleration voltage was set at 20 kV, and working distance was 12 mm).

5

Cell culture

Mouse 3T3 fibroblasts (from ATTC, Middlesex, UK) were cultured in DMEM supplemented with 10% fetal bovine serum, 2 mM L-glutamine, 100 U/ml penicillin, 100 μg/ml streptomycin (all from Invitrogen, Renfrewshire, UK). They were passaged upon reaching 80% confluency using trypsin-EDTA (Sigma-Aldrich, Dorset, UK) at a ratio of 1:3 and cultured on the scaffolds for 9 days prior to SEM.

Human osteosarcoma cell line Saos-2 cells (HTB-85 from ATTC) were cultured in 5% CO_2, 37°C in McCoys 5A medium with 15% fetal bovine serum, 2 mM L-glutamine, 100 U/ml penicillin, 100 μg/ml streptomycin (all from Invitrogen). They were passaged when confluent using trypsin-EDTA at a ratio of 1:3. They were modified to constitutively express GFP using retroviral integration. Briefly, phoenix-gag-pol (PGP) cells were transfected with 3 μg of pMX.GFP (Cell Biolabs, San Diego, CA, USA) and 3 μg of pVPack-VSV-G envelope protein (Strategene) using lipofectamine 2000 and Optimem media (both Invitrogen) according to the manufacturer's instructions. After 48 hrs viral supernatant was sterile filtered through a 0.45 μM filter (Nalgene) and added to Saos-2 cells. Three rounds of viral infection were carried out at 48 hour intervals which resulted in over 90% of Saos-2 cells expressing GFP.

Six lines of previously derived equine iPSCs[15,16] from three different horses were cultured on mitotically inactivated mouse embryonic fibroblasts in DMEM/F12, supplemented with: 15% FCS, 2 mM L-glutamine, 1% non-essential amino acids, 1 mM sodium pyruvate, 0.1 mM 2-mercaptoethanol (all Invitrogen), 1000 U/ml leukaemia inhibitory factor (LIF, Sigma), and 10 ng/ml basic fibroblast growth factor (bFGF, Peprotech, NJ, USA). Colonies were passaged mechanically every 5 to 7 days in the presence of 2 μM Thiazovivin (StemGent, Cambridge, MA).

Bone differentiation on the constructs was carried out in osteoblast differentiation media. This consisted of the iPSC base medium (lacking bFGF and LIF) or the Saos-2 base medium supplemented with 10 mM β-glycerophosphate, 50 μM ascorbic acid and 1 μM dexamethasone (all Sigma-Aldrich).

Prior to cell seeding the constructs were sterilised under UV light (10 minutes per side) and conditioned with the cell-type appropriate media overnight. 1x 10^4 cells were seeded onto each construct for all cell types. 3T3 and Saos-2 cells were seeded as single

6

cells and iPSCs were seeded as small colonies following mechanical passaging. Differentiation was carried out for 21 days with media replaced every 2-3 days.

Bone differentiation assays

To determine matrix mineralisation entire constructs were stained with von Kossa (Abcam, Cambridgeshire, UK) according to the manufacturer's instructions. Alizarin Red S staining for calcium deposition was performed by incubating the entire constructs with 2% Alizarin Red S pH 4.2 for 5 min. Hydroxyapatite deposition was detected using the OsteoImage bone mineralisation assay (Lonza, Berkshire, UK) according to the manufacturer's instructions. Alkaline phosphatase activity was measured using a quantitative colorimetric test on cell culture supernatant (Abcam) according to the manufacturer's instructions. Activity is measured in glycine units/ml where one glycine unit is the amount of enzyme causing the hydrolysis of one micromole of pNPP (p-nitrophenyl phosphate) per minute at pH 9.6 and 25°C.

RNA extraction, cDNA synthesis and qRT-PCR

RNA was extracted using Tri-reagent (Sigma-Aldrich), purified using the RNeasy mini kit (Qiagen, Manchester, UK) and treated with Ambion DNA-free (Life Technologies, Paisley, UK). cDNA was made from 1 μg of RNA using the sensiFAST cDNA synthesis kit (Bioline, London, UK). 2 μl aliquots of cDNA were used in qPCR. Primers were designed using NCBI Primer-Blast (https://www.ncbi.nlm.nih.gov/tools/primer-blast/). Primer sequences can be found in Table 1. qPCR was carried out using SYBR Green containing supermix (Bioline) on the Biorad C1000 Touch Thermal Cycler (Biorad, Hertfordshire, UK), and all PCR reactions performed in duplicate. PCR cycle parameters were 95°C for 10 min, followed by 40 cycles of 95°C for 15 seconds, 60°C for 15 seconds and 72°C for 15 seconds. At the end of the program a melt curve was produced by taking readings every 1°C from 65°C to 95°C. 18s rRNA levels did not change between treatments (data not shown) and was used to normalise gene expression using the $2^{-\Delta\Delta Ct}$ method [21].

Immunohistochemistry

This was performed on the entire constructs. The cells on the constructs were fixed in 3% paraformaldehyde for 20 min and permeabilised for 1h with 0.1% triton-X-100. They were washed in PBS and incubated with the primary antibodies overnight at 4°C before detection with an appropriate fluorescently labelled secondary antibody. All antibodies

7

were used at optimized concentrations in PBS and appropriate negative controls were performed using secondary antibodies alone and IgG matched to the host species, as well as specific isotype of the primary antibody. Coverslips were mounted using Vectashield Hardset mounting medium containing DAPI (4',6-diamidino-2-phenylindole, Vector Laboratories, Cambridge, UK). Primary antibodies included: mouse anti-collagen type I 1:100 (AB90395 Abcam, Cambridge, UK), mouse anti-osteonectin (SPARC) 1:20 (MAB941-100, Biotechne, Oxford, UK), mouse anti-osteopontin (SPP1) 1:50 (21742, Santa Cruz biotechnology, CA, USA), rabbit anti-bone sialoprotein (IBSP) 1:100 (ORB1100, Biorbyt, Cambridge, UK), rabbit anti-RUNX2 1:50 (10758, Santa Cruz), goat anti-osteocalcin (BGALP) 1:50 (18319, Santa Cruz). Secondary antibodies were goat anti-mouse alexafluor 594 1:200 (A11005, Invitrogen), goat anti-rabbit alexafluor 594 1:200 (A11012, Invitrogen) and rabbit anti-goat alexafluor 594 1:200 (Ab150144, Abcam). Constructs were inverted for imaging on a fluorescent microscope.

Results

Scaffold optimisation

To fit into a standard 24 well tissue culture plate, the optimal size which allowed the insertion and removal of constructs from the well while minimising the growth of cells under and around the construct was found to be 14.90 mm height, 14.90 mm width, thickness 1.66 mm (Figure 1).

The surface coating was optimised to ensure the maximum adherence and growth of cells on the surface. Scanning EM revealed the adherence of 3T3 cells within the meshwork of the scaffold (Figure 2A).

Two types of construct were tested; open constructs and closed constructs. The closed constructs had a fine mesh layer that coated the bottom of the construct, enclosing it as a more isolated unit for cell growth, whereas the open construct lacked this fine mesh layer, meaning cells were free to penetrate through the construct and adhere to the bottom of the cell culture plate (Figure 2B). Saos-2 cells expressing GFP were able to adhere to the scaffold of both construct types, but the open constructs with no mesh had far fewer cells remaining within the construct and many cells present on the bottom of the culture dish. In contrast the enclosed construct did not allow any cells to pass through to

8

the bottom of the culture dish. Enclosed constructs were therefore used in all further experiments.

iPSCs and Soas-2 cells differentiated on the 3D scaffold produce a mineralised matrix

GFP-labelled equine iPSCs were seeded as small colonies onto the constructs. These adhered to the constructs and individual cells migrated away from the colonies along the scaffold but after 21 days of differentiation the iPSC-derived cells were fewer in number and less evenly distributed than Saos-2 cells (Figure 3). Despite the ability of the cells to move through the pores, cells were attached throughout the depth of the scaffold (rather than just on the base of the enclosed construct). This can be seen in Figure 3 where the cells are clearly present on the scaffold layers containing pores of 450 μm.

Alizarin red S and von Kossa staining on the entire constructs demonstrated that calcium had been deposited by both Saos-2 and iPSCs following 21 days of culture in osteoblast differentiation medium (Figure 4 A and B). More intense and global staining of constructs seeded with Saos-2 cells was observed than in constructs seeded with iPSCs. Control constructs in which no cells had been seeded did not produce any positive staining.

Non-GFP labelled iPSCs were seeded onto constructs in osteoblast differentiation media for 21 days prior to fluorescent detection of hydroxyapatite. Clear deposition of hydroxyapatite could be visualised on the scaffold (Figure 4C). All Saos-2 cells used in these 3D studies were labelled with GFP and therefore we were not able perform fluorescent detection of hydroxyapatite on the Saos-2 seeded scaffolds.

iPSCs and Soas-2 cells differentiated on the 3D scaffold synthesise alkaline phosphatase

A low level of ALP activity was produced by undifferentiated iPSCs but the level of ALP activity increased over the 21 days of differentiation by 20.5 fold (Figure 5). This was still lower than the level of ALP activity for the Saos-2 cells which was 1.5 fold higher than for the iPSCs after 21 days of differentiation.

iPSCs differentiated on the 3D scaffold express osteoblast-associated genes and proteins

After 21 days of differentiation on the 3D scaffolds the iPSCs expressed the osteoblast associated genes *COL1A1* (collagen type I), *SPARC* (osteonectin), *RUNX2* (Runt Related Transcription Factor 2), *SPP1* (osteopontin) and *BGLAP* (osteocalcin), but no expression of *IBSP* (Integrin Binding Sialoprotein) was detected (Figure 6). Similarly,

9

immunohistochemical staining for osteoblast-associated proteins revealed positive, cell-associated staining for COL1A1, SPARC, RUNX2, SPP1 and BGALP but not IBSP (Figure 6). Gene and protein expression for the Saos-2 was not examined in this study.

Discussion

We have previously reported the successful 2D differentiation of equine iPSCs into osteoblasts[16] and here we report the use of a novel, thermoplastic 3D printed scaffold to allow *in vitro* 3D osteoblast differentiation of equine iPSCs.

The filament used to make the scaffolds is biocompatible[22], cheap to purchase and can be printed to any size or shape. Importantly, it is also optically transparent, whereas other printable polymers such as polylactide (PLA) and polycaprolactone (PCL) are opaque. . Here we optimised the scaffold fit to a standard 24 well tissue culture plate and performed oxygen etching to allow good adhesion of the cell types being tested. Without surface treatment cells do not attach to the Bendlay polymer. The polymer can be coated with other proteins such as fibronectin, collagen type I and laminin to promote cell adhesion (unpublished data), but we have only determined equine iPSC attachment and differentiation on oxygen etched polymers. This is a similar process to that performed in the manufacture of tissue culture plastics. We found that enclosed constructs containing a fine mesh layer on the base, retained the cells within the scaffold much more effectively than open scaffolds lacking the mesh layer, where many cells were found adhered to the bottom of the cell culture well. We did not test the use of ultra-low attachment culture plates in this work, but if open scaffolds are required (for example to improve blood vessel infiltration *in vivo*) low attachment plates may help encourage cell retention on the scaffolds rather than on the culture plate itself. Pores within the scaffold allow the diffusion of nutrients and cellular proliferation, migration and communication. A wide range of pore sizes have been used in bone tissue engineering, ranging from 20 μm to 1500 μm[23] and here we demonstrated that a combination of 150 μm and 400 μm provided an effective scaffold for *in vitro* differentiation and analysis.

Here we used scaffolds which were 1.66 mm thick and found that we had very good distribution of the cells throughout the depth of the scaffold. However, future work

10

to determine the effect of scaffold thickness on cell survival, migration and differentiation is required as the diffusion of nutrients may become limited as the thickness increases.

The transparency of the scaffold is of great benefit for *in vitro* studies as it allows the distribution and growth of the cells to be visualised during standard culture. How cells are distributed, proliferate and differentiate on a scaffold can all effect the likely functionality of the engineered tissue[24] and assessing this on non-transparent scaffolds requires additional techniques to be performed[25]. Furthermore, transparent scaffolds enable the use of the same protocols for the end point analysis of differentiation to be conducted as for 2D differentiation (e.g. immunocytochemical staining). Therefore, as a tool for studying *in vitro* bone differentiation this scaffold provides a cost-effective option that allows robust post-differentiation analyses to be performed.

Saos-2 cells seeded onto the constructs as single cells exhibited a very even distribution throughout the scaffold after 21 days of culture, whereas equine iPSCs, seeded as small colonies, were less well distributed after 21 days of culture and future work to enable the seeding of the iPSCs as single cells would likely be beneficial. Nevertheless, iPSCs did grow out of the original colonies along the meshwork of the scaffold. However, we were unable to find a successful method for extracting live cells from the scaffold to determine actual cell numbers at the end of the 21 days of differentiation. The extraction of live cells is likely complicated by the fact that upon differentiation into osteoblasts the cells produce a mineralised matrix[16].

We used both Alizarin red S and von Kossa staining to detect calcium production by the differentiated iPSCs and acknowledge that von Kossa reacts with the anionic portion of many salts and is not specific for calcium[26]. The iPSC-seeded constructs demonstrated distinct patches of calcium deposition, which may correlate with areas containing more cells, indicating successful osteoblast differentiation. Saos-2 seeded constructs were used as a positive control and had much more observable Alizarin red S and von Kossa staining which was evenly distributed across the constructs. This likely reflects the even distribution of the Saos-2 cells and the fact that as a human osteosarcoma cell line they readily undergo osteoblast differentiation to produce a mineralised matrix[27]. Non-GFP labelled equine iPSCs were also seeded on constructs and used to detect hydroxyapatite.

Clear deposition of hydroxyapatite was visible on the meshwork of the scaffold supporting conclusion that the iPSCs had differentiated into osteoblasts.

Bone mineralised requires the activity of alkaline phosphatase (ALP)[28] and we demonstrated that over the 21 days of differentiation there is an increase ALP activity. As we reported previously[16], and similar to human and mouse ESCs[29], undifferentiated equine iPSCs express a low level of ALP. ALP activity is increased approximately 20.5 fold after 21 days of differentiation in 3D. In comparison, we previously reported that ALP activity is only increased approximately 6 fold after 21 days of 2D differentiation[16], but we have not performed these experiments in parallel. ALP activity was only measured in one replicate of Saos-2 differentiation and so it was not possible to perform a statistical analysis, however, the level of ALP activity was higher in differentiating Saos-2 cells than iPSCs.

Quantitative PCR and immunohistochemistry produced matching results and demonstrated the expression of COL1A1, SPARC, SPP1, RUNX2 and BGALP by the differentiated equine iPSCs at both the gene and the protein level. Of note, the iPSCs that had grown out of the original colonies and existed as single cells on the scaffold were positive for the bone protein markers. This demonstrates that the migrating cells do undergo differentiation. However, no gene or protein expression was detected for IBSP. We have previously demonstrated that *IBSP* expression following 2D differentiation of equine iPSCs shows large amounts of inter-horse variability[16]. However, it may also reflect the fact that *IBSP (*bone sialoprotein) is a later marker of osteoblastic differentiation than the others that were tested[30,31]. RUNX2 is a key transcription factor in the osteoblast differentiation pathway[32,33] and has a relatively high expression after 21 days of iPSC differentiation. Similarly, *COL1A1* and *SPARC* have relatively high gene expression levels. These are upregulated in the early phases of differentiation[34,35] and are considered to be early markers of osteoblast differentiation[36-38]. In contrast, BGALP and SPP1 have lower expression levels and are both required in the later stages of bone formation[36,39,40]. Although these analyses were only performed on a single line of iPSCs and further replicates are required, they do suggest that the iPSCs may require additional time in culture to generate a more mature osteoblast phenotype. Alternatively, as the material used in the scaffold has been shown to affect the efficiency of bone differentiation of a

12

variety of cell types[17,41,42], coating the scaffold with osteogenic factors may lead to more efficient differentiation of the iPSCs.

Improving the efficiency of differentiation of iPSCs is particularly important with regard to their clinical application because any remaining undifferentiated cells may have the potential to undergo uncontrolled proliferation and tumour formation *in vivo*[43]. As we were not able to extract live cells from the scaffold, it was not possible to quantify the efficiency of differentiation of the iPSCs, for example using flow cytometry. Other methods using an intermediate differentiation step to mesenchymal stem cells (MSCs)[44] and removal of any undifferentiated iPSCs (using cell sorting) prior to 3D differentiation may help to reduce the safety concerns of using iPSC derived products clinically. Future work to determine the optimal duration of 3D differentiation is also required as in this study we only examined differentiation after 21 days.

These polycarbonate scaffolds are not biodegradable and would not break down over time *in vivo* in line with tissue healing. However, many non-biodegradable scaffolds/implants are used in *in vivo* fracture repair such as metals and PAA (polyacrylic acid)[45] and generally biodegradable scaffolds have poorer mechanical properties that can make them unsuitable for fracture repair in bones exposed to large forces[45,46]. The polycarbonate scaffolds used in this report can be easily scaled up and printed to any size or shape and can be fabricated rapidly. This would allow them to be custom produced to fit individual bone defects, whilst ensuring that the material, pore size etc remains standardised. Polycarbonate is lightweight but has a high tensile strength of 77 MPa and a high tensile break strength of 75-150% which means that it can withstand high loads and torsional stress far better than other thermoplastics which have been used in bone repair such as PLA (polylactide)[47] and PMMA (polymethyl methacrylate)[48]. This is of particular importance for equine clinical applications where limb bones are exposed to high loads and the native tissue has a high ultimate tensile strength of around 120 MPa[49].

In summary we report that equine iPSCs can be successfully differentiated into bone forming osteoblasts on a thermoplastic, 3D printed polymer which form the development of novel methods for improving fracture repair in horses in the future.

13

Acknowledgements

Author Disclosure Statement

No competing financial interests exist.

14

References

1   Morgan, R. & Dyson, S. Incomplete longitudinal fractures and fatigue injury of the proximopalmar medial aspect of the third metacarpal bone in 55 horses. *Equine Vet J* **44**, 64-70, doi:10.1111/j.2042-3306.2011.00371.x (2011).

2   Cahn, C. M. *The Merck Veterinary Manual.* (John Wiley & Sons, 2010).

3   Payne, R. J. & Compston, P. C. Short- and long-term results following standing fracture repair in 34 horses. *Equine Vet J* **44**, 721-725, doi:10.1111/j.2042-3306.2012.00569.x (2012).

4   Ma, J. *et al.* Concise review: cell-based strategies in bone tissue engineering and regenerative medicine. *Stem cells translational medicine* **3**, 98-107, doi:10.5966/sctm.2013-0126 (2014).

5   Boero, M. J. *et al.* Evaluation of the tibia as a source of autogenous cancellous bone in the horse. *Veterinary surgery : VS* **18**, 322-327 (1989).

6   RICHARDSON, G. L., POOL, R. R., PASCOE, J. R. & WHEAT, J. D. Autogenous Cancellous Bone Grafts From the Sternum in Horses Comparison With Other Donor Sites and Results of Use in Orthopedic Surgery. *Veterinary Surgery* **15**, 9-15, doi:doi:10.1111/j.1532-950X.1986.tb00166.x (1986).

7   Harriss, F. K., Galuppo, L. D., Decock, H. E., McDuffee, L. A. & Macdonald, M. H. Evaluation of a technique for collection of cancellous bone graft from the proximal humerus in horses. *Veterinary surgery : VS* **33**, 293-300, doi:10.1111/j.1532-950x.2004.04043.x (2004).

8   Jones, E. A., Giannoudis, P. V. & Kouroupis, D. Bone repair with skeletal stem cells: rationale, progress to date and clinical application. *Therapeutic advances in musculoskeletal disease* **8**, 57-71, doi:10.1177/1759720X16642372 (2016).

9   Perez, J. R. *et al.* Tissue Engineering and Cell-Based Therapies for Fractures and Bone Defects. *Frontiers in bioengineering and biotechnology* **6**, 105-105, doi:10.3389/fbioe.2018.00105 (2018).

10   McDuffee, L. A. *et al.* Osteoprogenitor cell therapy in an equine fracture model. *Veterinary surgery : VS* **41**, 773-783, doi:10.1111/j.1532-950X.2012.01024.x (2012).

15

11   Baird, A. E., Barsby, T. & Guest, D. J. Derivation of Canine Induced Pluripotent Stem Cells. *Reprod Domest Anim* **50**, 669-676. doi: 610.1111/rda.12562. Epub 12015 Jun 12512. (2015).

12   Kang, H., Shih, Y. V. & Varghese, S. Direct Conversion of Human Pluripotent Stem Cells to Osteoblasts With a Small Molecule. *Curr Protoc Stem Cell Biol* **44**, 1f.21.21-21f.21.26, doi:10.1002/cpsc.44 (2018).

13   Kang, H., Shih, Y. R., Nakasaki, M., Kabra, H. & Varghese, S. Small molecule-driven direct conversion of human pluripotent stem cells into functional osteoblasts. *Science advances* **2**, e1600691, doi:10.1126/sciadv.1600691 (2016).

14   Wu, Q. *et al.* Deriving Osteogenic Cells from Induced Pluripotent Stem Cells for Bone Tissue Engineering. *Tissue engineering. Part B, Reviews* **23**, 1-8, doi:10.1089/ten.TEB.2015.0559 (2017).

15   Bavin, E. P., Smith, O., Baird, A. E. G., Smith, L. C. & Guest, D. J. Equine induced pluripotent stem cells have a reduced tendon differentiation capacity compared to embryonic stem cells. *Frontiers in Veterinary Science* **2**, doi:10.3389/fvets.2015.00055 (2015).

16   Baird, A. *et al.* Osteoblast differentiation of equine induced pluripotent stem cells. *Biology Open*, doi:10.1242/bio.033514 (2018).

17   Polo-Corrales, L., Latorre-Esteves, M. & Ramirez-Vick, J. E. Scaffold design for bone regeneration. *Journal of nanoscience and nanotechnology* **14**, 15-56 (2014).

18   Shekaran, A. *et al.* Enhanced in vitro osteogenic differentiation of human fetal MSCs attached to 3D microcarriers versus harvested from 2D monolayers. *BMC Biotechnol* **15**, 102, doi:10.1186/s12896-015-0219-8 (2015).

19   Ravi, M., Paramesh, V., Kaviya, S. R., Anuradha, E. & Solomon, F. D. 3D cell culture systems: advantages and applications. *J Cell Physiol* **230**, 16-26, doi:10.1002/jcp.24683 (2015).

20   de Peppo, G. M. *et al.* Engineering bone tissue substitutes from human induced pluripotent stem cells. *Proceedings of the National Academy of Sciences of the United States of America* **110**, 8680-8685, doi:10.1073/pnas.1301190110 (2013).

21   Livak, K. J. & Schmittgen, T. D. Analysis of relative gene expression data using real time quantitative PCR and the $2^{-\text{deltadeltaCT}}$ Method. *Methods* **25**, 402-408 (2001).

16

22   Salentijn, G. I., Oomen, P. E., Grajewski, M. & Verpoorte, E. Fused Deposition Modeling 3D Printing for (Bio)analytical Device Fabrication: Procedures, Materials, and Applications. *Analytical chemistry* **89**, 7053-7061, doi:10.1021/acs.analchem.7b00828 (2017).

23   Loh, Q. L. & Choong, C. Three-dimensional scaffolds for tissue engineering applications: role of porosity and pore size. *Tissue engineering. Part B, Reviews* **19**, 485-502, doi:10.1089/ten.TEB.2012.0437 (2013).

24   Martin, I., Wendt, D. & Heberer, M. The role of bioreactors in tissue engineering. *Trends Biotechnol* **22**, 80-86, doi:10.1016/j.tibtech.2003.12.001 (2004).

25   Thevenot, P., Nair, A., Dey, J., Yang, J. & Tang, L. Method to analyze three-dimensional cell distribution and infiltration in degradable scaffolds. *Tissue engineering. Part C, Methods* **14**, 319-331, doi:10.1089/ten.tec.2008.0221 (2008).

26   Bonewald, L. F. *et al.* von Kossa staining alone is not sufficient to confirm that mineralization in vitro represents bone formation. *Calcified tissue international* **72**, 537-547, doi:10.1007/s00223-002-1057-y (2003).

27   McQuillan, D. J., Richardson, M. D. & Bateman, J. F. Matrix deposition by a calcifying human osteogenic sarcoma cell line (SAOS-2). *Bone* **16**, 415-426 (1995).

28   Golub, E. E. & Boesze-Battaglia, K. The role of alkaline phosphatase in mineralization. *Curr Opin Orthop* **18**, 444-448 (2007).

29   Stefkova, K., Prochazkova, J. & Pachernik, J. Alkaline Phosphatase in Stem Cells. *Stem Cells International* **2015** (2015).

30   Mayr-Wohlfart, U., Fiedler, J., Gunther, K. P., Puhl, W. & Kessler, S. Proliferation and differentiation rates of a human osteoblast-like cell line (SaOS-2) in contact with different bone substitute materials. *J Biomed Mater Res* **57**, 132-139, doi:10.1002/1097-4636(200110)57:1<132::AID-JBM1152>3.0.CO;2-K [pii] (2001).

31   Bouleftour, W. *et al.* The role of the SIBLING, Bone Sialoprotein in skeletal biology - Contribution of mouse experimental genetics. *Matrix biology : journal of the International Society for Matrix Biology* **52-54**, 60-77, doi:10.1016/j.matbio.2015.12.011 (2016).

17

32   Graneli, C. *et al.* Novel markers of osteogenic and adipogenic differentiation of human bone marrow stromal cells identified using a quantitative proteomics approach. *Stem Cell Res* **12**, 153-165, doi:S1873-5061(13)00135-9 [pii] 10.1016/j.scr.2013.09.009 [doi] (2014).

33   Huang, W., Yang, S., Shao, J. & Li, Y. P. Signaling and transcriptional regulation in osteoblast commitment and differentiation. *Front Biosci* **12**, 3068-3092, doi:2296 [pii] (2007).

34   Jikko, A., Harris, S. E., Chen, D., Mendrick, D. L. & Damsky, C. H. Collagen integrin receptors regulate early osteoblast differentiation induced by BMP-2. *Journal of bone and mineral research : the official journal of the American Society for Bone and Mineral Research* **14**, 1075-1083, doi:10.1359/jbmr.1999.14.7.1075 (1999).

35   Jundt, G., Berghauser, K. H., Termine, J. D. & Schulz, A. Osteonectin--a differentiation marker of bone cells. *Cell and tissue research* **248**, 409-415 (1987).

36   Köllmer, M., Buhrman, J. S., Zhang, Y. & Gemeinhart, R. A. Markers Are Shared Between Adipogenic and Osteogenic Differentiated Mesenchymal Stem Cells. *Journal of developmental biology and tissue engineering* **5**, 18-25, doi:10.5897/JDBTE2013.0065 (2013).

37   Rosset, E. M. & Bradshaw, A. D. SPARC/osteonectin in mineralized tissue. *Matrix biology : journal of the International Society for Matrix Biology* **52-54**, 78-87, doi:10.1016/j.matbio.2016.02.001 (2016).

38   Mundlos, S., Schwahn, B., Reichert, T. & Zabel, B. Distribution of osteonectin mRNA and protein during human embryonic and fetal development. *J Histochem Cytochem* **40**, 283-291, doi:10.1177/40.2.1552170 (1992).

39   Zoch, M. L., Clemens, T. L. & Riddle, R. C. New insights into the biology of osteocalcin. *Bone* **82**, 42-49, doi:10.1016/j.bone.2015.05.046 (2016).

40   Weinreb, M., Shinar, D. & Rodan, G. A. Different pattern of alkaline phosphatase, osteopontin, and osteocalcin expression in developing rat bone visualized by in situ hybridization. *Journal of bone and mineral research : the official journal of the American Society for Bone and Mineral Research* **5**, 831-842, doi:10.1002/jbmr.5650050806 (1990).

18

41   Mayr-Wohlfart, U., Fiedler, J., Gunther, K. P., Puhl, W. & Kessler, S. Proliferation and differentiation rates of a human osteoblast-like cell line (SaOS-2) in contact with different bone substitute materials. *J Biomed Mater Res* **57**, 132-139 (2001).

42   Ataie, M., Shabani, I. & Seyedjafari, E. Surface mineralized Hybrid Nanofibrous Scaffolds Based On Poly(L-lactide) and Alginate Enhances Osteogenic Differentiation of Stem Cells. *Journal of biomedical materials research. Part A*, doi:10.1002/jbm.a.36574 (2018).

43   Liu, Z. *et al.* The tumourigenicity of iPS cells and their differentiated derivates. *J Cell Mol Med* **17**, 782-791, doi:10.1111/jcmm.12062 (2013).

44   Lepage, S. I. *et al.* Generation, Characterization, and Multilineage Potency of Mesenchymal-Like Progenitors Derived from Equine Induced Pluripotent Stem Cells. *Stem Cells Dev* **25**, 80-89, doi:10.1089/scd.2014.0409 (2016).

45   Ghassemi, T. *et al.* Current Concepts in Scaffolding for Bone Tissue Engineering. *The archives of bone and joint surgery* **6**, 90-99 (2018).

46   Sheikh, Z. *et al.* Biodegradable Materials for Bone Repair and Tissue Engineering Applications. *Materials (Basel, Switzerland)* **8**, 5744-5794, doi:10.3390/ma8095273 (2015).

47   Dorati, R. *et al.* Biodegradable Scaffolds for Bone Regeneration Combined with Drug-Delivery Systems in Osteomyelitis Therapy. *Pharmaceuticals (Basel, Switzerland)* **10**, 96, doi:10.3390/ph10040096 (2017).

48   Shimko, D. A. & Nauman, E. A. Development and characterization of a porous poly(methyl methacrylate) scaffold with controllable modulus and permeability. *Journal of biomedical materials research. Part B, Applied biomaterials* **80**, 360-369, doi:10.1002/jbm.b.30605 (2007).

49   Evans, G. P., Behiri, J. C., Vaughan, L. C. & Bonfield, W. The response of equine cortical bone to loading at strain rates experienced in vivo by the galloping horse. *Equine Vet J* **24**, 125-128 (1992).

19

Reprint Author

Dr Deborah Guest, Centre for Preventive Medicine, Animal Health Trust, Lanwades Park,

Kentford, Newmarket, Suffolk, CB8 7UU, UK

20

Table 1 Primer sequences for equine gene transcripts.

Gene	Forward	Reverse
18S	CCCAGTGAGAATGCCCTCTA	TGGCTGAGCAAGGTGTTATG
COL1A1	TGCGAAGACACCAAGAACTG	GACTCCTGTGGTTTGGTCGT
SPARC	TGGCGAGTTTGAGAAGGTGT	TTTGCAAGGCCCGATGTAGT
SPP1	AGCCCCAGGAAAAATCGCTG	GGCATAAGCAAATCACGGCA
IBSP	GGACTGCACACGGAAACAATC	ACAGGCCATTCCCAAAATGC
RUNX2	CCAAGTGGCAAGGTTCAACG	AACTCTTGCCTCGTCCACTC
BGALP	GTCTCGGGGGTTCCAAGGTTA	AATCTCTGGTAGCTGTGTTGGT

21

Figure legends
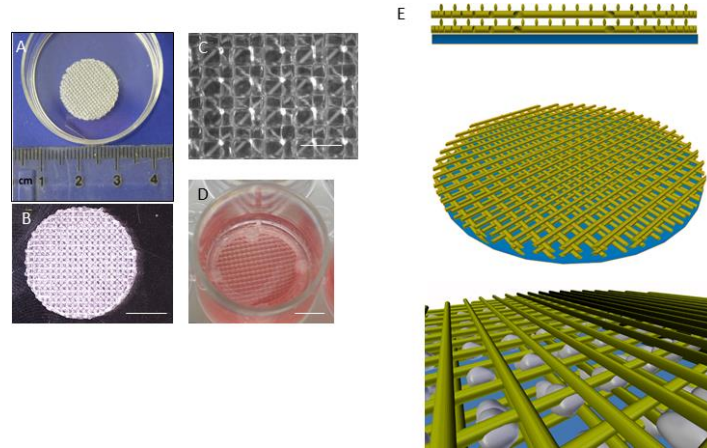
Figure 1. The 3D scaffolds can be printed to fit into a standard 24 well tissue culture plate. A) Photograph of the scaffold construct showing bulk size. B) Photograph of the scaffold demonstrating that it is transparent. Scale bar = 5 mm. C) Micrograph showing a magnified view of the scaffold to demonstrate the scaffold pores. Scale bar = 1200 μm. D) Photograph of the scaffold in culture conditions. Scale bar = 5 mm. E) A conceptual schematic of the scaffolds with the filament shown in yellow, the mesh layer in blue and cells represented in grey.
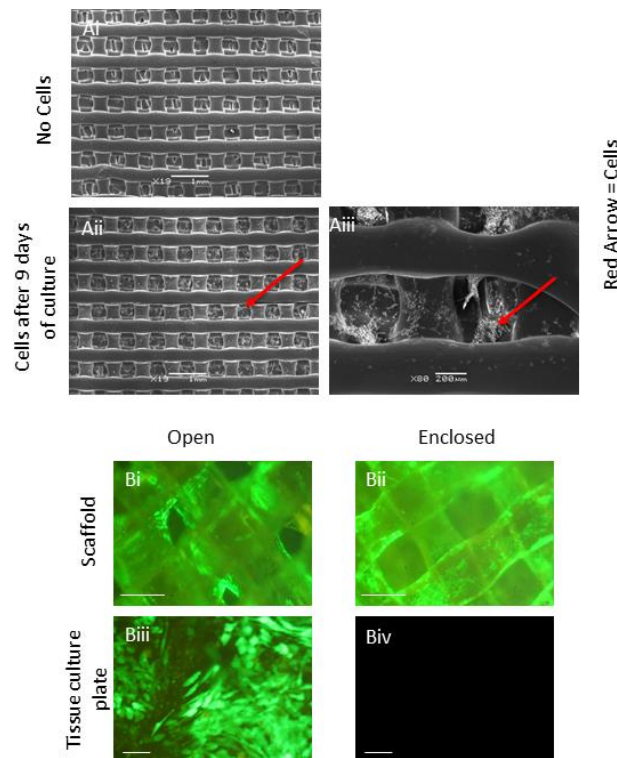
Figure 2. 3T3 mouse fibroblasts and human Soas-2 cells can attach and proliferate to the 3D scaffolds. A) SEM of the scaffold in the absence (i) and presence (ii and iii) of 3T3 cells after 9 days of culture. The red arrow highlights attached cells. B) GFP labelled Saos-2 cells grow better on enclosed scaffolds than open scaffolds. Soas-2 cells adhere to the both open (i) and enclosed (ii) scaffolds but large numbers of cells pass through the open scaffolds onto the base of the tissue culture plate in the open (iii) but not the enclosed (iv) scaffolds. Scale bar in i and ii = 400 μm. Scale bar in iii and iv = 30 μm.
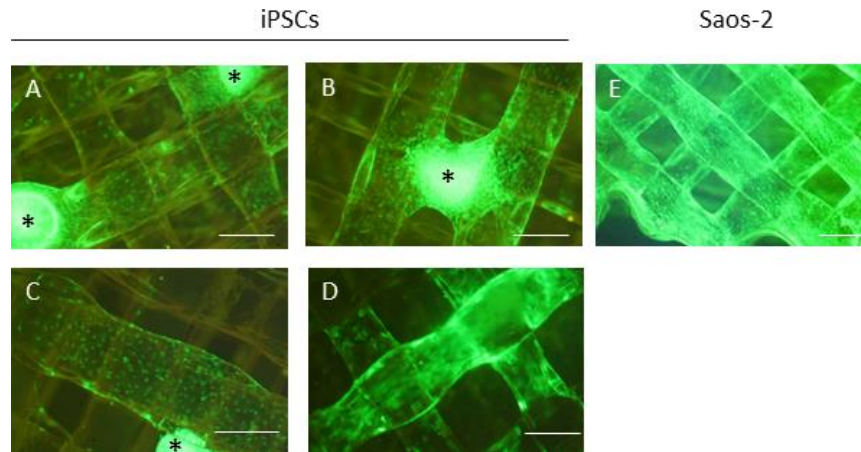
23

Figure 3. GFP labelled iPSCs seeded as colonies and differentiated for 21 days on the 3D scaffold. iPSC colonies (indicated by *) adhere to the scaffold and cells migrate out along the scaffold fibres (A - D). However, after 21 days of culture, iPS-derived cells are fewer in number and less evenly distributed than Saos-2 cells (E). Four images of the iPSCs are provided to demonstrate the heterogeneity in their distribution. A single representative image of a scaffold seeded with Saos-2 is shown as these cells were homogenously distributed. Scale bar = 400 µm.

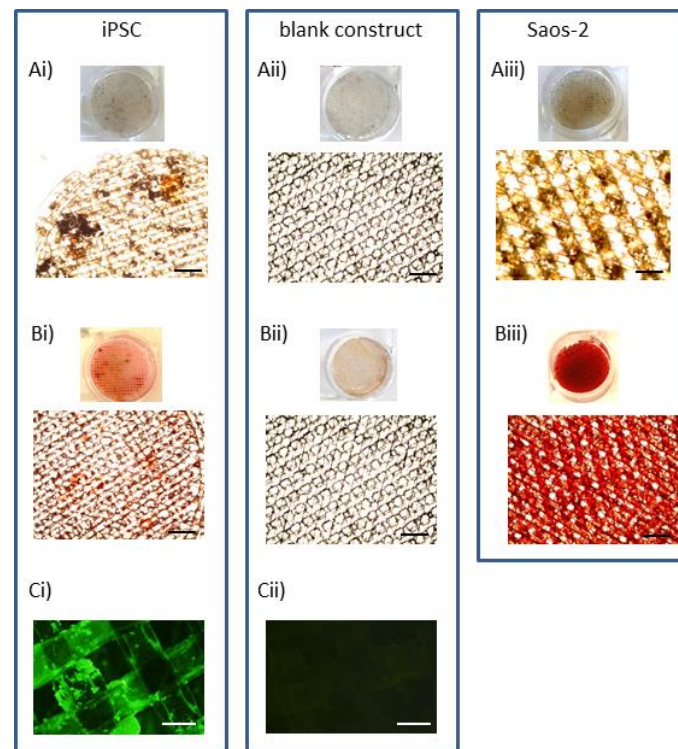

Figure 4. iPSCs differentiated on the 3D scaffold produce a mineralised matrix. A) von Kossa staining for calcium on constructs seeded with i) iPSCs, ii) no cells (blank construct) or iii) Saos-2 cells. Positive staining is shown in black/brown. B) Alizarin red S staining for calcium with positive staining shown in red. Scale bar in A and B = 1200 μm. C) Hydroxyapatite staining with deposits fluorescing green. iPSC images are representative of four replicates using four independent clonal iPSCs derived from two different horses. Scale bar in C = 400 μm.
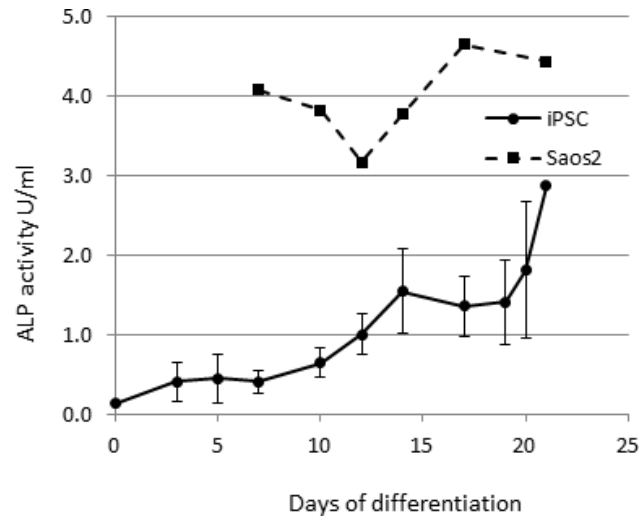
25

Figure 5. iPSCs differentiated on the 3D scaffold have increasing alkaline phosphatase activity (ALP) with time. Error bars represent the standard error of the mean from a total of six clonal lines of iPSCs derived from three different horses. ALP from on replicate of Saos-2 cells differentiated on the 3D scaffold was measured as a positive control.
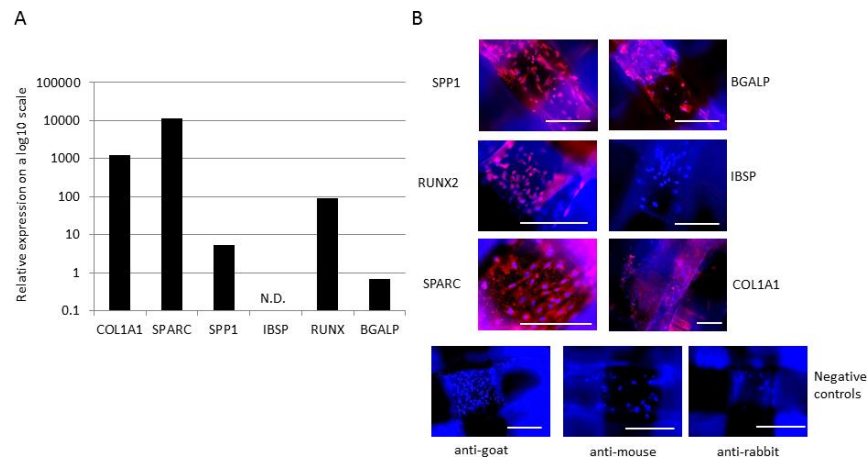
Figure 6. iPSCs differentiated on the 3D scaffolds for 21 days express osteoblast associated genes and proteins. A) Relative gene expression (on a log10 scale) of osteoblast associated genes. N.D. = expression not detected. B) Differentiated iPSCs express detectable levels of all osteoblast proteins except for IBSP. Scale bars = 400 μm.